2013

Krill biomass and aggregation structure in relation to tidal cycle in a penguin foraging region off the Western Antarctic Peninsula

KS Bernard
Virginia Institute of Marine Science

DK Steinberg
Virginia Institute of Marine Science

ICES Journal of Marine Science

ICES Journal of Marine Science (2013), 70(4), 834–849. doi:10.1093/icesjms/fst088

Krill biomass and aggregation structure in relation to tidal cycle in a penguin foraging region off the Western Antarctic Peninsula

Kim S. Bernard[1,2]* and Deborah K. Steinberg[1]

[1]*Virginia Institute of Marine Science, College of William & Mary, P.O. Box 1346, Gloucester Point, VA, 23062, USA*
[2]*College of Earth, Ocean, and Atmospheric Sciences, Oregon State University, 104 Ocean Admin Bldg, Corvallis, OR, 97331, USA*

**Corresponding Author: College of Earth, Ocean, and Atmospheric Sciences, Oregon State University, Corvallis, OR, USA. tel: 541 737 9337; fax: 541 737 2064; e-mail: kbernard@coas.oregonstate.edu*

Bernard, K. S., and Steinberg, D. K. 2013. Krill biomass and aggregation structure in relation to tidal cycle in a penguin foraging region off the Western Antarctic Peninsula. – ICES Journal of Marine Science, 70: 834–849

Antarctic krill are a key component of the diet of Adélie penguins inhabiting the Western Antarctic Peninsula (WAP), yet our understanding of the variability of krill distribution patterns within nearshore penguin feeding grounds is limited. A recent study of the foraging patterns of penguins breeding in the northern WAP suggests that tidal phase plays a role in foraging distance. We used acoustics to examine biomass and aggregation structure of krill in the penguin foraging grounds off Palmer Station during diurnal and semi-diurnal tides. Nearshore, integrated krill biomass during diurnal tides was significantly higher than during semi-diurnal tides. Krill aggregations were also shallower, closer together, and larger in dimension during diurnal tides. Conversely, krill aggregations had higher volumetric biomass and abundance during semi-diurnal tides. Further offshore, at the head of the Palmer Deep canyon, krill aggregations were similar to those observed nearshore during diurnal tides (i.e. shallow, close together, and large in dimension). Since krill aggregation structure strongly influences availability as a potential prey source, we suggest that foraging behavior of Adélie penguins in this region is strongly linked to the variability in nearshore krill aggregation structure as well as biomass.

Keywords: acoustics, Adélie penguin, aggregation structure, Antarctic krill, Adélie penguin, distribution patterns.

Introduction

Antarctic krill (*Euphausia superba*) play a fundamental role in the pelagic ecosystem of the Southern Ocean: as a primary food item for many of the region's top predators (Laws, 1977; Wienecke *et al.*, 2000; Nicol *et al.*, 2008), as an important grazer of phytoplankton (Perissinotto *et al.*, 1997; Ross *et al.*, 1998; Bernard *et al.*, 2012), and as a predator of microzooplankton and copepods (Price *et al.*, 1988; Atkinson and Snÿder, 1997; Schmidt *et al.*, 2006). Antarctic krill form a major component in the diet of Adélie penguins (*Pygoscelis adeliae*), particularly during the breeding season when adult penguins rely on the availability of krill within their foraging range to feed their chicks (Wienecke *et al.*, 2000; Fraser and Hofmann, 2003; Nicol *et al.*, 2008). The reproductive success of Adélie penguins has been directly linked to krill densities and demographics, with years of low krill abundance corresponding with reduced chick fledging weights (Nicol *et al.*, 2008; Chapman *et al.*, 2010).

Distribution patterns of Antarctic krill are highly variable, as a number of biological (top-down and bottom-up) and physical (currents, sea surface temperature, sea ice dynamics) drivers influence the dynamics of krill populations over space and time (Trathan *et al.*, 2003; Siegel, 2005; Loeb *et al.*, 2009; Wiebe *et al.*, 2011). At larger spatial and temporal scales (100s to 1000s of km and seasons to years, respectively), Antarctic krill distribution patterns and densities may be affected by the extent of annual sea ice, seawater temperature, and phytoplankton biomass (Brierley *et al.*, 1997; Lascara *et al.*, 1999; Brierley *et al.*, 1999). At smaller spatial and temporal scales (10s of km and days), the dynamics of Antarctic krill communities may be influenced by the interaction of localized currents and topography (Santora and Reiss, 2011), and meteorological events such as storms (Warren *et al.*, 2009). Euphausiid communities in the northern hemisphere are similarly affected by currents and topography (Mackas *et al.*, 1997; Lavoie *et al.*, 2000; Cotté and Simard, 2005). It is well documented that sub-mesoscale variability in Antarctic krill densities and aggregation structure has an impact on the foraging behavior of top predators, including whales, seabirds, penguins and seals (Hunt *et al.*, 1992; Mori and Boyd, 2004; Santora *et al.*, 2009; Warren *et al.*, 2009; Santora *et al.*, 2010; Santora and Reiss, 2011). An improved understanding of the sub-mesoscale variability in Antarctic krill populations is thus critical to better interpret changes in the population and foraging dynamics of their predators.

In the nearshore waters off Palmer Station, southern Anvers Island, foraging patterns of breeding Adélie penguins are correlated with tidal phase (Oliver *et al.*, 2013). During diurnal tides, penguins forage close to shore, within 6 km of their breeding site on Humble Island (64°46'S 64°06'W). As the tidal phase switches to semi-diurnal, the penguins remain close to shore for the first four days, but then begin to move further off, into the head of the Palmer Deep canyon, approximately 12 km away. Adélie penguins breeding in this region feed primarily on Antarctic krill (Fraser and Hofmann, 2003). As predator foraging behavior is closely linked with prey availability and distribution patterns (Alonzo *et al.*, 2003), variability in Adélie foraging behavior likely reflects variability in the distribution patterns and densities of Antarctic krill. We hypothesized that nearshore Antarctic krill densities would be greater during diurnal tides, and that the krill prey field would be more favorable for penguin foraging during those periods. The objectives of this study were to (i) examine the variability of nearshore Antarctic krill densities and distribution patterns with respect to tidal phase, and (ii) compare these with patterns observed at the head of the Palmer Deep canyon.

Methods

Study site and sampling protocol

We conducted this study in the vicinity of Anvers Island Western Antarctic Peninsula (Figure 1) during the 2011–2012 austral summer. For the nearshore tidal component of the study an acoustic grid survey was conducted from small boats (Zodiacs) in the waters off Palmer Station during both diurnal and semi-diurnal tidal phases (see Figure 2 for an example of the tidal variability observed during the study). The grid was selected to fall within the 6 km diurnal foraging ranges of Adélie penguins breeding on Humble Island (Figure 1). The grid consisted of two sub-grids; each comprised of six transects ranging between 1.5 and 1.75 km, with a total grid length of 25.4 km. Four sets of diurnal and semi-diurnal tidal series were sampled between 20 November 2011 and 15 January 2012. During that period we were able to conduct the full grid survey in 17 days (nine diurnal tides and eight semi-diurnal tides). Adélie penguin foraging data (not presented herein) can be found in the study of Oliver *et al.* (2013), part of which was conducted within the same season and region as our study.

The Palmer Deep acoustic survey was conducted on board the RV "Laurence M. Gould" on 4 January 2012 (corresponding to a diurnal tidal phase nearshore). The survey grid was comprised of four transects, each approximately 8.5 km in length and 1.3 km apart (Figure 1), with a total length of 38 km.

Antarctic krill length frequencies

Antarctic krill were collected for length-frequency analysis using a 2-mm mesh, 1-m diameter ring net towed obliquely from the Zodiac through krill aggregations. Only when aggregations of Antarctic krill were very dense ($>$3000 ind. m^{-3}), could be visually observed from the surface, and were large (i.e. height $>$ 20 m and length $>$ 100 m) were we able to successfully sample them with the net (two net tows were conducted in this instance). We also collected Antarctic krill for length measurements from the RV "Laurence M. Gould" from three net tows using a 750 μm mesh, 2 × 2-m square frame Metro net towed obliquely along transects of the Palmer Deep grid (Figure 1). Though different net types and mesh sizes were used, there were no discernible differences observed in length frequencies of krill collected with the two nets. Length measurements were made for a subsample of at least 100 *E. superba* randomly selected from the catch, using Standard Length 1 (SL1) for total length according to Mauchline (1980). Measured krill were categorized according to length, ranging from 10–65 mm in 1-mm increments. During our study, the majority of krill sampled fell within the 10–25 mm size range (Figure 3), representing a strong year-0 recruit.

Krill target strength estimates

We used the Distorted-Wave Born Approximation (DWBA) model of Lawson *et al.* (2006) to predict target strengths (TS) for selected length categories of Antarctic krill. The model was parameterized in part with measured values and in part with values obtained from the literature. Krill length categories (derived from net tows described above) ranged from 8–65 mm and were divided into 1-mm increments. Lengths were converted to SL2 from SL1 using the equations provided in Lawson *et al.* (2006). The ratio of length to cylindrical radius was calculated from net samples and a mean value of 9.5 was used. The regression equations used to calculate acoustic material properties (g and h) were obtained from Chu and Wiebe (2005). The model was set to estimate TS for the mean of a range of orientations, where a mean of 20° and standard deviation of 20° were selected following Lawson *et al.* (2004) and Chu *et al.* (1993). TS (units of decibels relative to 1 m^2) was then used to calculate backscattering cross-section $\langle\sigma_{bs}\rangle$ where

$$\mathrm{TS} = 10\log_{10}(\sigma_{bs}). \quad (1)$$

Acoustic data collection and processing

A single frequency (120 kHz) Biosonics DT-X scientific echosounder was used to conduct the acoustic surveys. The echosounder was towed horizontally at a depth of ~1 m at speeds of 3–5 knots. The system was calibrated prior to the study by the manufacturer and again in the field, using a standard target (a tungsten carbide calibration sphere provided by the manufacturer). A maximum observation depth of 250 m was achieved with a ping rate of 1 ping per second. Volume backscattering strength (Sv) measurements were binned vertically into 1-m depth bins and horizontally into 5-ping (~8 m) bins. Krill were then identified from other possible sources of scattering where volume backscattering strength at 120 kHz exceeded the − 70 dB threshold.

An element in the acoustic matrix that qualified as krill, based on the above criteria, was considered part of an aggregation if any of its eight neighbouring elements also had qualified as krill (Lawson *et al.*, 2008b). Neighbouring elements classified as krill were grouped into aggregations using the Image Processing Toolbox in MATLAB (R2013a). Euclidean distances between elements in a matrix considered krill were computed. Neighbouring elements with a Euclidean distance ≤ 1 were considered to be within the same aggregation. Each krill aggregation was allocated a unique identifying number. All aggregations were then visually examined and compared to the corresponding echograms. All incorrectly classified aggregations (i.e. elements that qualified as krill but were likely other scatterers, such as fish or macrobenthic algae, or were the result of noise in the acoustic backscatter) were flagged and excluded from further analyses.

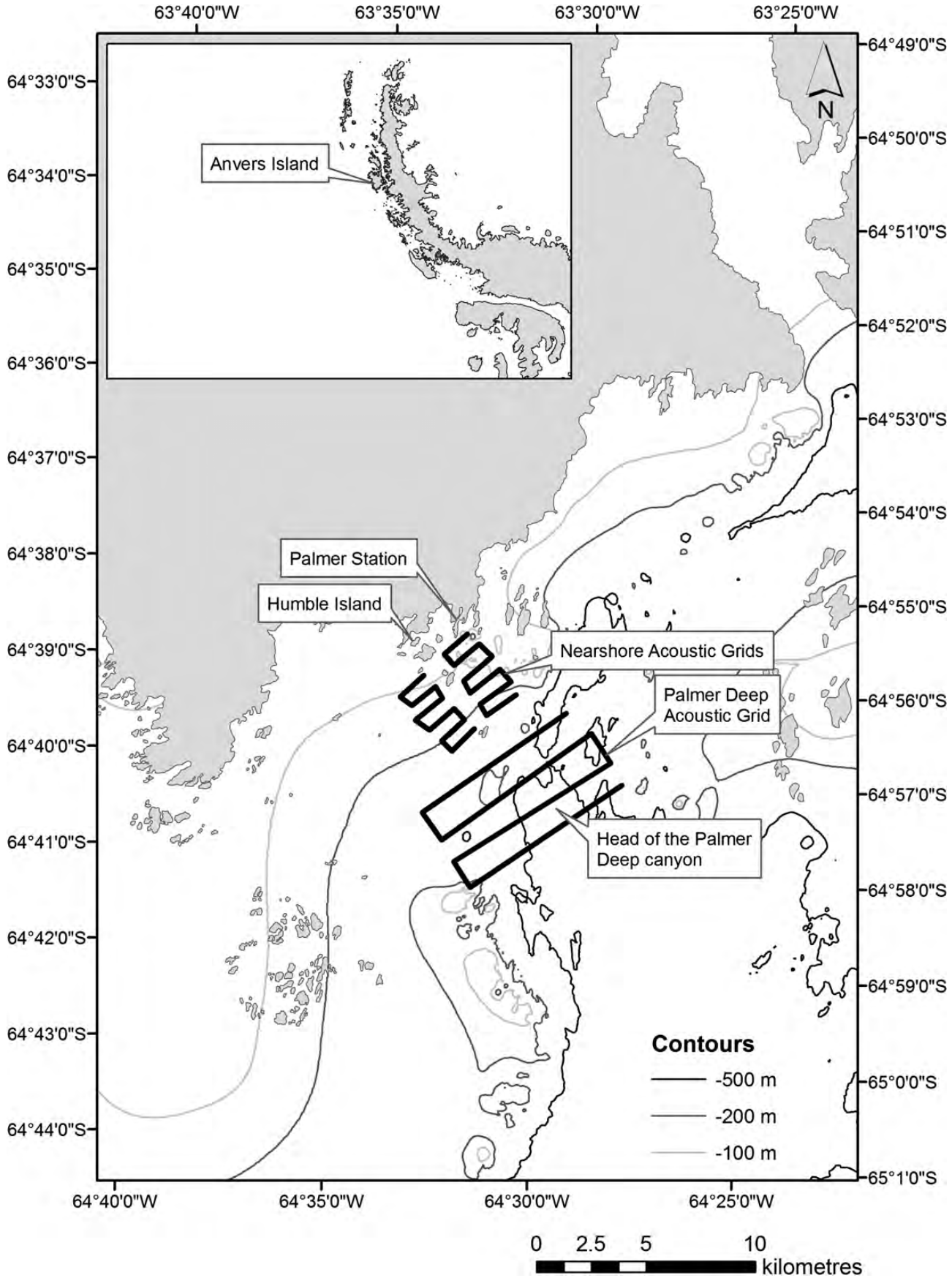

Figure 1. Map of the study area, showing the nearshore and head of the Palmer Deep canyon acoustic grids. Palmer Station (located on Anvers Island), Humble Island, and the Palmer Deep canyon are highlighted. Inset shows the Antarctic Peninsula with Anvers Island highlighted.

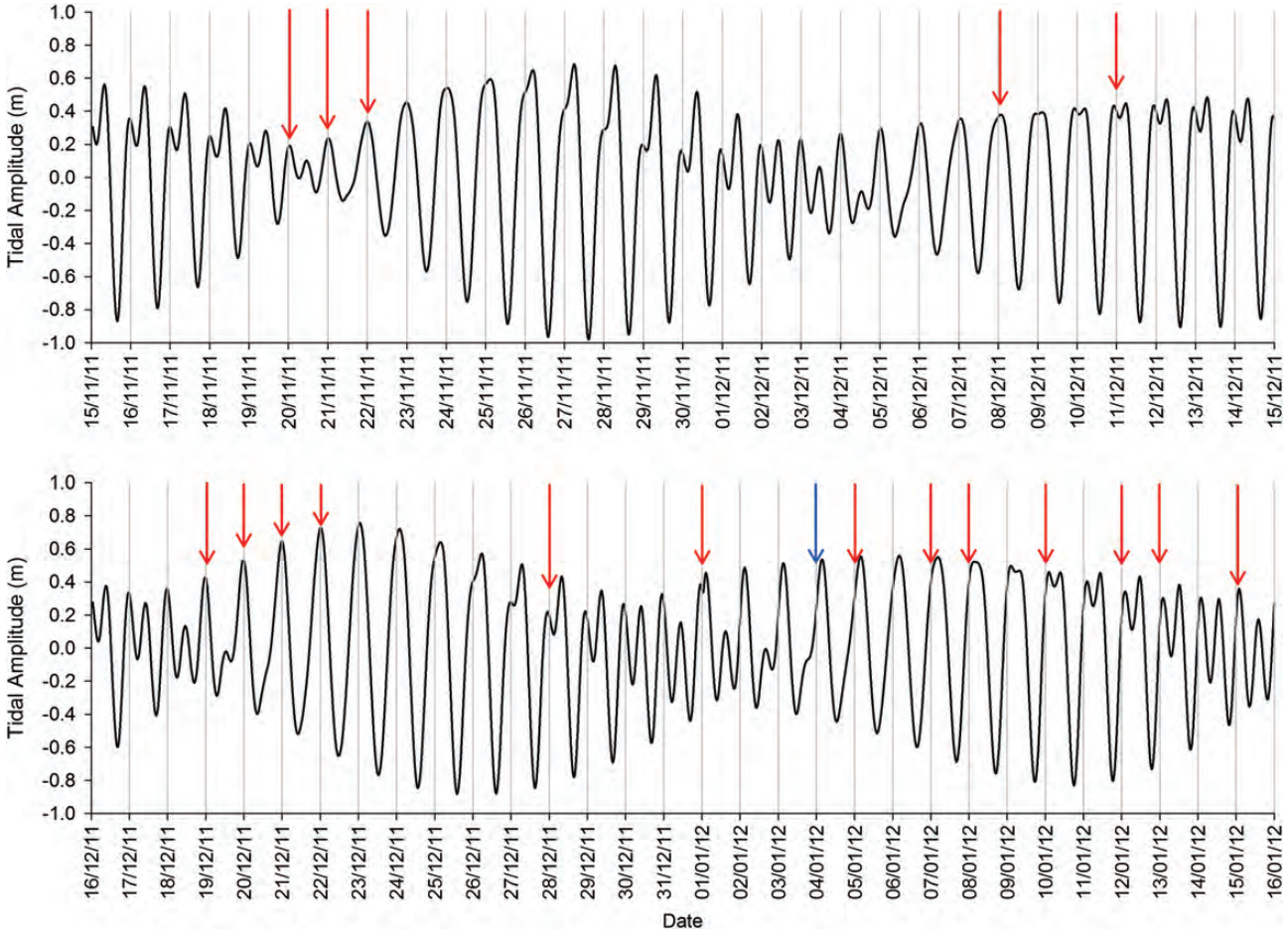

Figure 2. Diurnal and semi-diurnal tidal phases during this study. Semi-diurnal tides are those for which two high and two low tides occur each day, while diurnal tides have only a single high and low tide per day. Grey vertical grid-lines represent days. Red arrows indicate nearshore survey days; the blue arrow indicates the single survey day (1 April 2012) at the head of the Palmer Deep canyon.

Krill abundance and biomass estimates

Krill abundance (ind. m^{-3}) and biomass (g m^{-3}) were determined following the methods described in Lawson *et al.* (2004, 2008b). (Details provided in online Supplementary Data for the present publication.) Krill biomass was integrated over the water column (0 m to the sea floor or 0–250 m where bottom depth was deeper than 250 m) for each horizontal bin to convert values to g m^{-2}. Integrated biomass values at each horizontal bin were then averaged across both grids to estimate the mean integrated biomass for the region on a particular day.

Krill aggregation parameters

Identified krill aggregations (see Acoustic data collection and processing) were examined in further detail. Mean depth (m) of each aggregation was calculated as the centre point on the vertical plane. Aggregation height (m) was measured as the difference between the deepest and shallowest depth bin of a particular aggregation, and length (m) calculated as the distance between the start and end coordinates of a particular aggregation. The ratio of length to height was calculated for each aggregation. The distances between each aggregation and every other aggregation encountered on a particular day were determined as the distance from the end-point of one aggregation to the starting point of another, and the nearest neighbor distances (NND, m) were calculated as the shortest distance between an aggregation and any other aggregation. Binned biomass estimates were integrated over the depth of each aggregation to obtain aggregation-specific integrated biomass estimates (g m^{-2}). Depth-integrated biomass was then horizontally integrated for each aggregation to obtain aggregation-specific biomass encounter rates (kg m^{-1}). Mean volumetric biomass (g m^{-3}) and abundance (ind. m^{-3}) estimates for each aggregation were calculated to determine the packing density of a given aggregation.

Statistical analyses

Our primary objective was to determine if there were significant differences in krill distribution patterns and biomass nearshore during periods when Adélie penguins forage close to shore, compared with when they forage at the head of the Palmer Deep canyon. As Adélie penguins typically forage close to shore during diurnal tides and offshore during semi-diurnal tides (Oliver *et al.*, 2013), we compared nearshore krill distribution and biomass between the two tidal phases. However, observations of foraging Adélie penguins in the region (Oliver *et al.*, 2013) indicate that foraging birds remain nearshore for the first four days of a semi-diurnal tide (thereafter moving further offshore). Because of this "lag", we categorized two of our sampling days (12 November 2011 and 1 October 2012) that fell

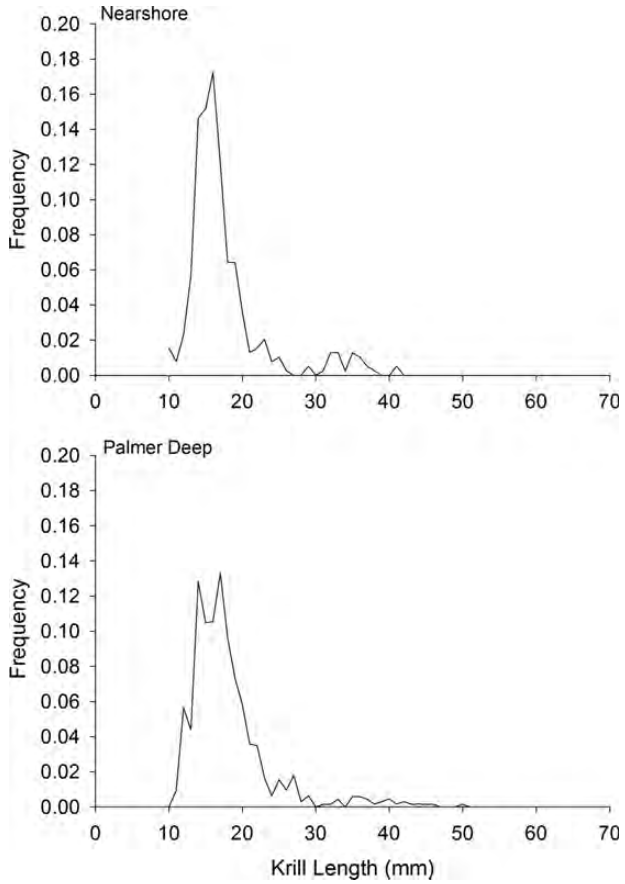

Figure 3. Length frequencies of Antarctic krill collected nearshore and at the head of the Palmer Deep canyon. Length frequencies are based on measurements made from a sub-sample of 257 krill from two net tows conducted nearshore, and 585 krill from three net tows at the head of the Palmer Deep canyon. Data are binned in 1-mm increments from 10–64 mm.

on the second day of a semi-diurnal tide as "diurnal" days instead of "semi-diurnal" days for our statistical analyses. A comparison of nearshore with offshore krill distribution patterns and biomass, although only from a single survey conducted during a diurnal tide, provides some indication of the prey field at the alternate Adélie penguin feeding grounds.

Daily variability in mean depth-integrated krill densities nearshore was assessed using a Kruskal–Wallis One Way Analysis of Variance on Ranks. Mean depth-integrated krill densities were compared between tidal phases in the nearshore (i.e. diurnal versus semi-diurnal tides – NS-D and NS-SD, respectively) and between the nearshore and the head of the Palmer Deep canyon (PD) using Kruskal–Wallis One Way Analysis of Variance on Ranks.

We identified the presence of distinct aggregation types using a Principle Components Analysis (PCA) and a Partitioning Around Medoids (PAM) cluster analysis, after Kaufman and Rousseeuw (1990). First, the PCA was carried out on centred and normalized krill aggregation parameters. The PAM cluster analysis was then performed on the results of the PCA. Since in all partitioning methods of cluster analysis the number of clusters (k) must be set *a priori*, we used the silhouette method of validation to select the most appropriate number for k (Kaufman and Rousseeuw 1990). Eigenvectors of the first three principle components were used to identify key aggregation parameters; where the absolute value of an eigenvector element was greater than the product of 0.7 and the maximum absolute eigenvector value for a given principle component the parameter was considered to have a significant influence (Cox *et al.*, 2011). Kruskal–Wallis One Way Analysis of Variance on Ranks tests were used to examine variability in aggregation parameters for each identified aggregation type between NS-D, NS-SD and PD.

A Chi-square test was used to examine the variability in the relative contribution of identified aggregation types to tidal phase (diurnal versus semi-diurnal) and to region (nearshore versus Palmer Deep).

Results

Krill biomass

Nearshore krill biomass as related to tidal phase

Integrated krill biomass in the nearshore waters off Palmer Station varied significantly from day to day during tidal cycles ($p < 0.001$), ranging from a mean of 9 g m^{-2} on 8 December 2011 to 329 g m^{-2} on 7 January 2012 (Figure 4). But overall, nearshore mean integrated krill biomass was significantly higher during diurnal tides than during semi-diurnal tides ($p < 0.001$, $Q = 21.997$, Figure 5). The lowest recorded daily krill biomass was observed during a diurnal tide (8 December 2011); however, northerly winds in excess of ~35 knots persisted for two days prior to 8 December, and we assume that this resulted in a net advection of the upper water-column offshore from our study region (T. Miles, pers. comm.), potentially transporting the krill with it. While krill biomass was generally low during semi-diurnal tides, elevated biomass was observed on the semi-diurnal tide on 10 January 2012, which was the second day of the fourth semi-diurnal tidal phase. Krill biomass on this day was not significantly different from that observed during the previous diurnal tide ($p > 0.05$), suggesting that biomass had not yet begun to drop off.

Difference between nearshore and head of the Palmer Deep canyon

Mean integrated krill biomass was significantly higher over the head of the Palmer Deep canyon than it was nearshore during semi-diurnal tides ($p < 0.05$). However, during diurnal tides, krill biomass was statistically greater nearshore than over the head of the Palmer Deep ($p < 0.05$, Figure 5).

Krill aggregation structure

Aggregation types

The highest Silhouette Coefficient (SC), 0.66, was calculated for $k = 2$. Consequently, with $k = 2$ as one of the input parameters, the PAM cluster analysis identified two distinct aggregation types. Type 1 aggregations had smaller dimensions ($p < 0.001$ for both aggregation height and length) than Type 2 aggregations (Table 1). There was no significant difference in the mean depth of Type 1 and Type 2 aggregations ($p = 0.094$, Table 1). Type 2 aggregations had significantly higher abundances and biomass of krill ($p < 0.001$ for volumetric abundance and biomass, and for aggregation-specific integrated biomass), but were further apart from each other, i.e. had greater NNDs than Type 1 aggregations ($p < 0.001$, Table 1). Biomass encounter rate was significantly higher for Type 2 aggregations ($p < 0.001$, Table 1). There was no significant difference in the mean distance between the Humble Island penguin nesting site and Type 1 and Type 2 krill aggregations ($p = 0.479$, Table 1). Aggregation-specific integrated biomass and biomass

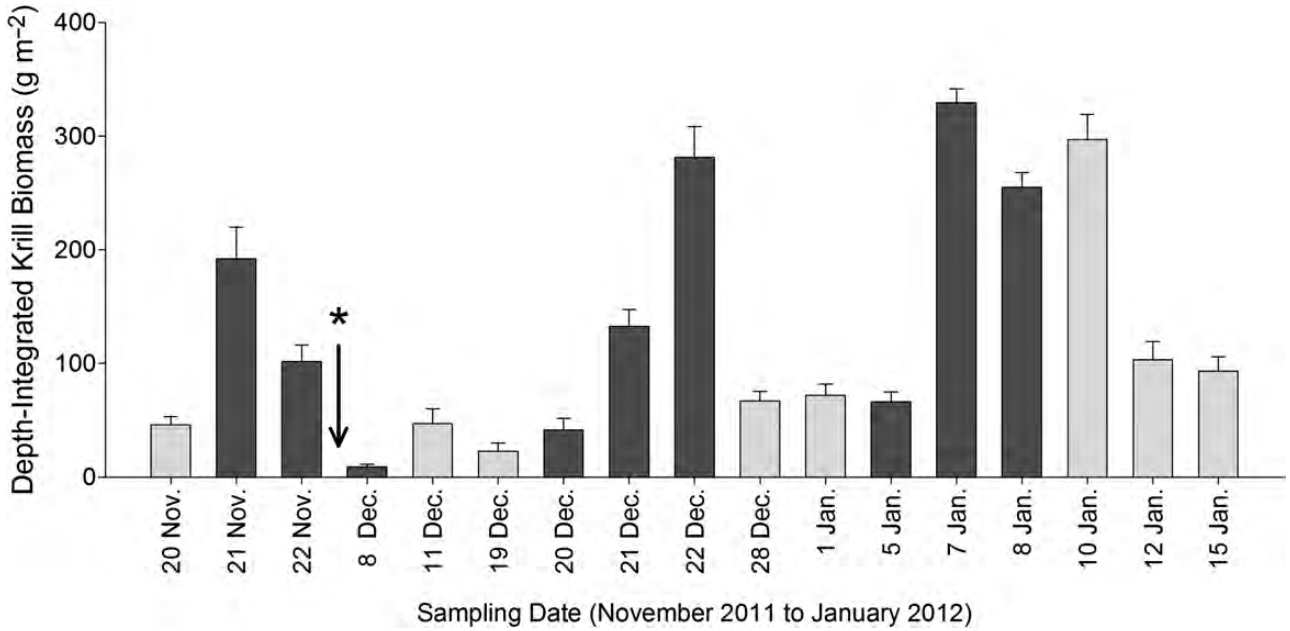

Figure 4. Mean daily depth-integrated krill biomass (g m^{-2}) during diurnal (dark grey) and semi-diurnal (pale grey) tides during austral summer 2011–2012. The asterisk marks the occurrence of a two-day, gale-force northerly wind. Error bars indicate standard errors.

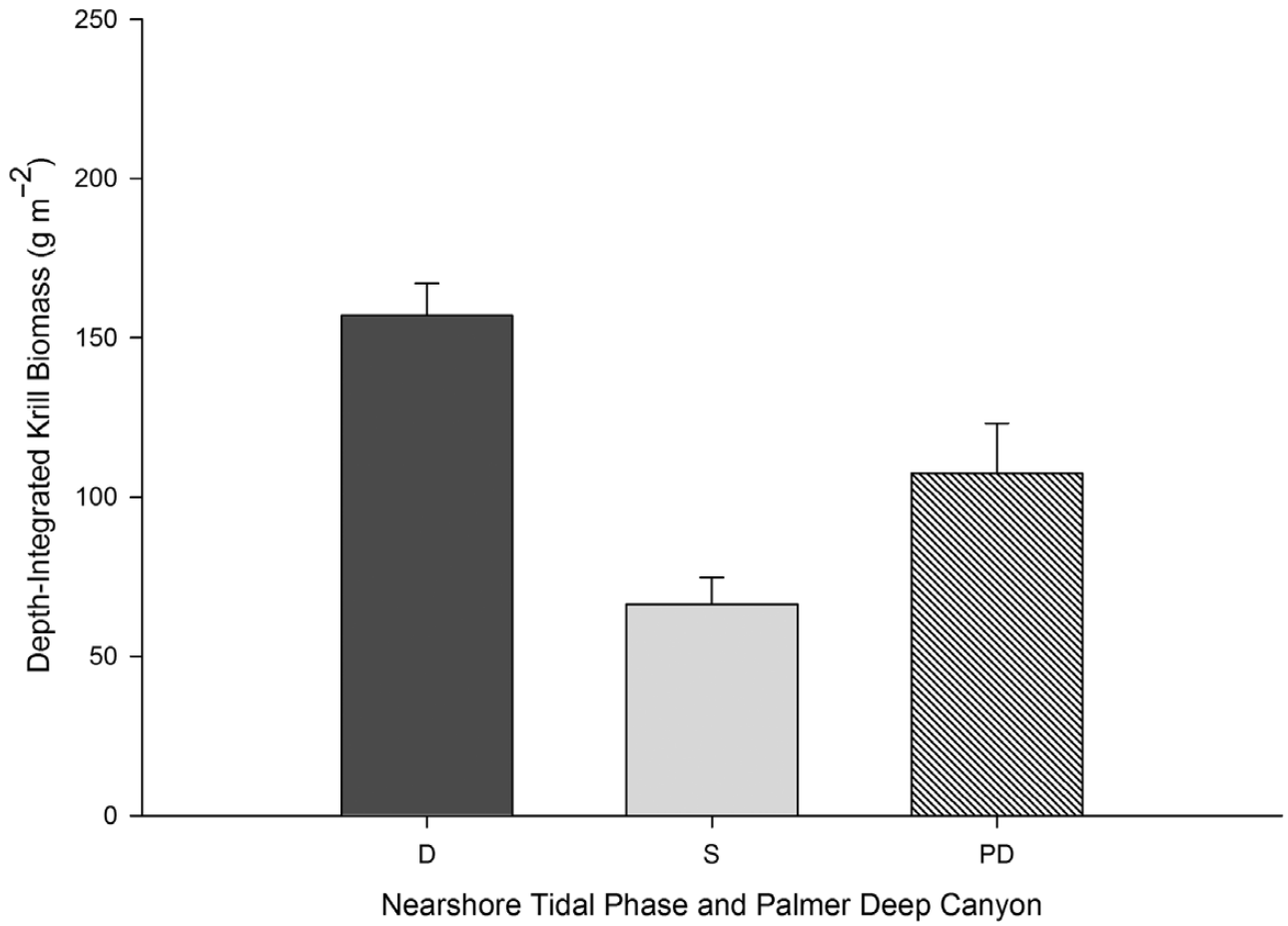

Figure 5. Mean depth-integrated krill biomass (g m^{-2}) for all nearshore diurnal (D, dark grey) and semi-diurnal (S, pale grey) tides, and for the head of the Palmer Deep canyon (PD, diagonal hatch). Error bars indicate standard errors.

Table 1. Variability in mean aggregation parameters (standard deviation in parentheses) between Type 1 and Type 2 aggregations identified with Principle Component Analysis and Partitioning Around Medoids Analysis.

	Type 1		Type 2				
Aggregation Parameter	**(n = 774)**		**(n = 564)**		**PC1 (79.94%)**	**PC2 (9.38%)**	**PC3 (3.87%)**
Depth (m)	38.2	(29.3)	34.9	(26.1)	0.02	−0.04	0.10
Height (m)	3.7	(2.4)	11.3	(7.9)	−0.15	0.19	−0.06
Length (m)	23.5	(20.1)	114.2	(425.1)	−0.16	0.39	**0.46**
L:H	7.2	(6.1)	9.1	(20.0)	−0.01	0.20	**0.52**
NND (m)	25.6	(13.6)	49.0	(34.1)	−0.08	0.17	0.10
Dist. Humble (km)	2960.9	(1015.9)	2868.2	(977.0)	0.004	0.17	−0.25
Vol. Ab. (ind. m^{-3})	28.9	(27.3)	580.5	(787.0)	−0.39	**− 0.75**	**0.43**
Vol. Bio. (g m^{-3})	2.4	(2.3)	46.8	(63.4)	−0.38	−0.14	−0.33
Int. Bio. (g m^{-2})	13.8	(14.4)	671.0	(1144.8)	**−0.49**	−0.005	**− 0.36**
Bio. Enc. Rate (kg m^{-1})	0.4	(0.5)	87.8	(339.1)	**−0.65**	0.38	0.09

L:H = length-to-height ratio, NND = nearest neighbor distance, Dist. Humble = distance from penguin nesting site on Humble Island, Vol. Ab. = volumetric abundance, Vol. Bio. = volumetric biomass, Int. Bio. = depth-integrated biomass (integrated over the height of the aggregation), Bio. Enc. Rate = biomass encounter rate. Eigenvectors for the first three principle components (PC1–PC3) are provided for each aggregation parameter. The percent variation explained by each principle component is given in parentheses. Aggregation parameters with significant influence (in bold) were determined as eigenvector elements (u_{ij}), where $|u_{ij}| > 0.7 \max(|u_j|)$.

Table 2. Percent contribution of aggregation Types 1 and 2 to total aggregations encountered nearshore during different tidal phases, and offshore at the head of the Palmer Deep canyon.

	Type 1	Type 2
Nearshore Diurnal	41	59
Nearshore Semi-Diurnal	43	57
Offshore Palmer Deep	46	54

encounter rate dominated the variance along PC1, while volumetric abundances dominated PC2 (Table 1). Length, length-to-height ratio, volumetric abundance, and aggregation-specific integrated biomass accounted for most of the variance of PC3 (Table 1). There was no significant difference in the frequency of occurrence of Type 1 and Type 2 aggregations between either the diurnal and semi-diurnal tides or the nearshore and Palmer Deep canyon ($p = 0.490$ Chi-square analysis, Table 2).

Nearshore aggregation characteristics as related to tidal phase

Type 1 aggregations did not vary significantly in dimension during diurnal tides vs. during semi-diurnal tides; however, they were significantly closer together during diurnal tides (shorter NNDs, Table 3, Figures 6 and 7). In comparison, Type 2 aggregations were significantly larger in dimension during diurnal tides than during semi-diurnal tides, though there was no significant difference in NND between tidal phases (Table 4, Figures 6 and 7). Both aggregation types were significantly shallower during diurnal tides than during semi-diurnal tides (Tables 3 and 4, Figure 6). There was no significant difference in the mean distance between Humble Island and krill aggregations encountered during either diurnal or semi-diurnal tides (Tables 3 and 4). Volumetric abundance and biomass and aggregation-specific integrated biomass of krill did not vary significantly between tidal phases for either aggregation type (Tables 3 and 4, Figures 8 and 9). Biomass encounter rates did not vary between tidal phases for Type 1 aggregations, but were significantly higher during diurnal tides for Type 2 aggregations (Tables 3 and 4, Figure 9).

Difference between nearshore and head of the Palmer Deep canyon

Overall, the shallowest aggregations were encountered at the head of the Palmer Deep canyon (Tables 3 and 4, Figure 6). Type 1 aggregations occurring at the head of the Palmer Deep canyon were statistically longer than those occurring nearshore during either diurnal or semi-diurnal tides, and their length-to-height ratios were also different between the two locations (Table 3, Figure 7). Type 2 aggregations were narrower in height at the head of the Palmer Deep canyon than those observed nearshore during diurnal tides, but were similar in dimension to those observed nearshore during semi-diurnal tides (Table 4, Figure 7). Aggregations at the head of the Palmer Deep canyon were statistically further apart from one another than those observed nearshore (greater NNDs, Tables 3 and 4, Figure 6). Volumetric biomass of Type 1 aggregations was highest at the head of the Palmer Deep canyon, while volumetric abundance was lowest in this region (Table 3, Figure 8). Both volumetric abundance and biomass of Type 2 aggregations were significantly lower at the head of the Palmer Deep canyon than nearshore during either tidal phase (Tables 3 and 4, Figure 8). Aggregation-specific integrated biomass and biomass encounter rates of Type 1 aggregations were highest at the head of the Palmer Deep canyon (Table 4, Figure 9). Aggregation-specific integrated biomass and biomass encounter rate of Type 2 aggregations was significantly lower at the head of the Palmer Deep canyon than nearshore during diurnal tides, but no difference was observed between the head of the canyon and nearshore during semi-diurnal tides (Table 4, Figure 9).

Discussion

Krill biomass

Historical data for penguin foraging distances show that Adélie penguins forage nearshore within 6 km of the breeding site during diurnal tides, and during the first four days of a semi-diurnal tide. Subsequently they move farther afield, foraging at the head of the Palmer Deep canyon approximately 10 km away (Oliver *et al.*, 2013). We found that mean depth-integrated krill biomass nearshore was significantly higher during diurnal tides than during semi-diurnal tides, suggesting that nearshore krill biomass might

Table 3. Results of the pair-wise multiple comparison procedure (Dunn's Method) following the Kruskal–Wallis One Way Analysis of Variance on Ranks for Type 1 aggregations.

	NEARSHORE – SEMI-DIURNAL	OFFSHORE – PALMER DEEP
NEARSHORE – DIURNAL	**Depth − Q = 3.565**	**Depth − Q = 2.938**
	Height − NS	Height − NS
	Length − NS	**Length − Q = 4.059**
	L:H − NS	**L:H − Q = 4.211**
	NND − Q = 2.820	**NND − Q = 6.507**
	Dist. Humble − NS	**Dist. Humble − Q = 13.389**
	Vol. Ab. − NS	**Vol. Ab. − Q = 13.495**
	Vol. Bio. − NS	**Vol. Bio. − Q = 3.181**
	Int. Bio. − NS	**Int. Bio. − Q = 2.816**
	Bio. Enc. Rate − NS	**Bio. Enc. Rate − Q = 3.785**
NEARSHORE – SEMI-DIURNAL		**Depth − Q = 4.823**
		Height − NS
		Length − Q = 4.507
		L:H − Q = 3.274
		NND − Q = 4.201
		Dist. Humble − Q = 12.287
		Vol. Ab. − Q = 11.647
		Vol. Bio. − Q = 3.532
		Int. Bio. − Q = 3.697
		Bio. Enc. Rate − Q = 4.659

L:H = length-to-height ratio, NND = nearest neighbour distance, Dist. Humble = distance to the nesting site on Humble Island, Vol. Ab. = aggregation volumetric abundance, Vol. Bio. = aggregation volumetric biomass, Int. Bio. = biomass integrated over depth of aggregation, Bio. Enc. Rate = biomass encounter rate. Q statistic values are given for significant results ($p < 0.05$), in bold. NS = not significant.

be locally enhanced through tidal currents and that Adélie penguins respond to these changes in their foraging. Diurnal tides (typically 1–1.5 m amplitude) in the region have greater amplitude than semi-diurnal tides (typically 0.5–1 m amplitude) (Figure 2) and might directly transport krill accumulating at the head of the Palmer Deep canyon into the nearshore waters off Palmer Station, where they may become entrained. It is well documented that submarine canyons result in considerable enhancement of productivity (Klinck, 1996), and euphausiids in particular accumulate in dense aggregations at the head of canyons (Mackas *et al.*, 1997; Lavoie *et al.*, 2000; Allen *et al.*, 2001; Genin, 2004; Santora and Reiss, 2011). During our study, we observed high krill biomass at the head of the Palmer Deep canyon; however, it was not as high as that recorded nearshore during diurnal tides, suggesting that accumulated biomass of krill at the head of the canyon may be further concentrated by tidal currents interacting with local bathymetry nearshore.

Krill abundance and biomass are highly variable and this is made apparent through synoptic plots such as those of Lawson *et al.* (2008a) and Warren and Demer (2010), which show krill densities ranging from <1 to over 10 000 g m^{-2}. During our study, integrated krill biomass at the head of the Palmer Deep canyon ranged from <1 to $\sim$4000 g m^{-2}, while that in the nearshore ranged between 1 and $\sim$20 000 g m^{-2} during diurnal tides and between 1 and $\sim$16 000 g m^{-2} during semi-diurnal tides.

In addition to the direct advection of krill into nearshore waters, it is possible that diurnal tidal currents may transport warmer Upper Circumpolar Deep Water (UCDW) from over the shelf of the WAP into nearshore waters (Martinson *et al.*, 2008; Martinson and McKee, 2012), delivering nutrients and increasing water-column stratification, thereby increasing phytoplankton productivity. Once nearshore, UCDW water may become trapped by local bathymetry and currents, allowing a suitable residence time for the formation of phytoplankton blooms and the subsequent increase in primary consumers, which may in turn attract higher trophic levels, including krill.

Possible sources of error

In order to accurately quantify krill biomass or abundance from acoustic data, precise knowledge on the length frequencies of krill within any given aggregation is required. Since it was only possible to sample a subset of the aggregations from the Zodiac during our acoustic surveys, we assumed a length-frequency distribution based on this subset for the region and applied those data to our acoustic analyses. The biomass and abundance estimates provided here are thus more qualitative than quantitative and are not intended for use in krill fisheries management. However, these estimates are valuable for examining the krill prey field in the nearshore waters off Palmer Station, allowing us to gain insight into the distribution patterns and aggregation structure of krill in the nearshore.

The different net-mouth opening and mesh sizes of the two nets used for collecting krill for length-frequency measurements may have introduced error. The smaller mouth opening of the 1-m ring net towed from the Zodiac may have led to greater net avoidance and perhaps undersampling of larger krill compared with the larger mouth net (reviewed in Sameoto *et al.*, 2000; although see Wiebe *et al.*, 1982). However, the smaller mouth net had a larger mesh size to reduce clogging caused by elevated phytoplankton biomass nearshore and which would increase water flow-through and reduce wake. All tows were performed during the day, and while this could lead to greater visual avoidance of the net, the bias would be in the same direction for both net types. Regardless, both nets yielded similar krill length frequencies.

Smaller individuals ($<$20 mm) dominated the regional krill population during our investigation. In order to estimate the potential source of error incurred from the use of a krill length frequency

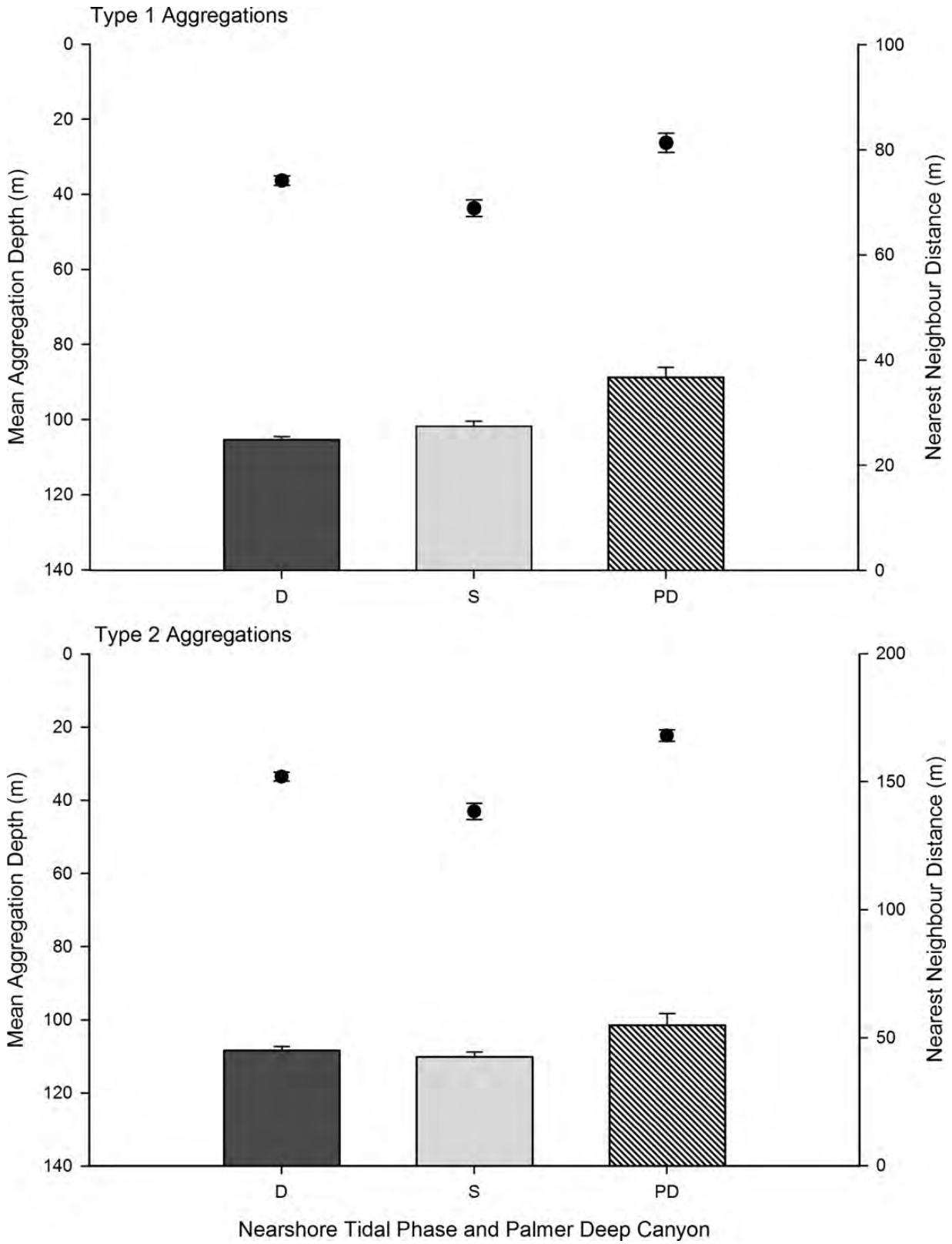

Figure 6. Mean aggregation depths (m, represented by black circles) for nearshore diurnal (D) and semi-diurnal (S) tides and for the head of the Palmer Deep canyon (PD) for Type 1 (top panel) and Type 2 (bottom panel) aggregations. Mean nearest neighbour distance (m, represented by bars) for nearshore diurnal (dark grey) and semi-diurnal (pale grey) tides, and for the head of the Palmer Deep canyon (diagonal hatch). Error bars indicate standard errors.

Table 4. Results of the pair-wise multiple comparison procedure (Dunn's Method) following the Kruskal-Wallis One Way Analysis of Variance on Ranks for Type 2 aggregations.

	NEARSHORE – SEMI-DIURNAL	OFFSHORE – PALMER DEEP
NEARSHORE – DIURNAL	**Depth − Q = 3.104**	**Depth − Q = 4.398**
	Height − Q = 4.587	**Height − Q = 3.438**
	Length − Q = 4.615	Length − NS
	L:H − NS	L:H − NS
	NND − NS	**NND − Q = 2.831**
	Dist. Humble − NS	**Dist. Humble − Q = 17.648**
	Vol. Ab. − NS	**Vol. Ab. − Q = 16.535**
	Vol. Bio. − NS	**Vol. Bio. − Q = 3.529**
	Int. Bio. − NS	**Int. Bio. − Q = 3.514**
	Bio. Enc. Rate − Q = 2.668	**Bio. Enc. Rate − Q = 3.436**
NEARSHORE – SEMI-DIURNAL		**Depth − Q = 6.224**
		Height − NS
		Length − NS
		L:H − NS
		NND − Q = 2.469
		Dist. Humble − Q = 14.271
		Vol. Ab. − Q = 14.830
		Vol. Bio. − Q = 3.291
		Int. Bio. − NS
		Bio. Enc. Rate − NS

L:H = length-to-height ratio, NND = nearest neighbour distance, Dist. Humble = distance to the nesting site on Humble Island, Vol. Ab. = aggregation volumetric abundance, Vol. Bio. = aggregation volumetric biomass, Int. Bio. = biomass integrated over depth of aggregation, Bio. Enc. Rate = biomass encounter rate. Q statistic values are given for significant results ($p < 0.05$), in bold. NS = not significant.

dominated by juveniles, we applied a krill length frequency dominated by larger individuals (obtained from Adélie penguin stomach samples, W. Fraser, unpublished data) to our acoustic data analysis and compared those results with results presented above. When length frequencies were skewed towards smaller individuals (as in our study), estimated volumetric abundances were 7.5 times higher than those determined from populations dominated by larger individuals (mean = 259 and 35 ind. m^{-3}, respectively; *t*-test; $p < 0.001$; $t = -13\,427$). Expectedly, volumetric biomass estimates were less affected by changing krill length frequency. The population dominated by smaller individuals had an estimated 1.3 times greater volumetric biomass than that dominated by larger individuals (mean = 16 g m^{-3} and mean = 21 g m^{-3}, respectively; *t*-test; $p = 0.07$; $t = -2.7$).

Krill aggregation structure

We identified two distinct aggregation types, Type 1 and Type 2, during our study, which corresponded well with aggregation types identified by Tarling *et al.* (2009). Our Type 1 aggregations were similar in size to the Type 1a aggregations identified by Tarling *et al.* (2009) and referred to as *small swarms*. Our Type 1 aggregations were, however, far more densely packed than Type 1a aggregations in Tarling *et al.* (2009): 29 ind. m^{-3} vs. 6.5 ind. m^{-3}, respectively. Likewise, our Type 2 aggregations were similar in size to Tarling *et al.* (2009) Type 2a aggregations (their *large swarms*), but again our aggregations were more densely packed than theirs: 581 ind. m^{-3} vs. 65 ind. m^{-3}, respectively. There are two possible reasons why our aggregations had higher packing densities: krill size and proximity to the coast. First, the predominant krill cohort during our study was the year zero cohort, with krill <20 mm in length. In contrast, krill lengths recorded by Tarling *et al.* (2009) ranged between 20 and 60 mm. Krill target strength increases with increasing body length (Lawson *et al.*, 2006, and references therein), thus in order to produce a given acoustic backscattering cross-section, smaller individuals would need to be more numerous than larger ones. Another possible reason for the higher concentrations of krill in our study could be that we sampled primarily in the shallow (<250 m depth) coastal waters within 6 km of the shoreline, whereas Tarling *et al.* (2009) covered a considerably larger area (encompassing South Georgia Island, the South Sandwich Islands, the South Orkney Islands, and the northern tip of the Antarctic Peninsula) and much of their acoustic sampling occurred some distance from the land. If tides and other currents locally concentrate krill nearshore, then we would expect to see higher packing densities of krill in nearshore aggregations compared with offshore aggregations.

Cox *et al.* (2011) also identified aggregation types in an acoustic study of krill around South Georgia. While our Type 2 aggregations were similar in dimension and packing density to their Type 2 aggregations, our Type 1 aggregations did not match with any of the three aggregation types identified in that study (Cox *et al.*, 2011).

Quality of the krill prey field

Differences in the structure of krill aggregations have an impact on the quality of the aggregations as a food source (Mori and Boyd, 2004; Cox *et al.*, 2011). We chose to define the quality of a krill aggregation by its *availability* and its *energy value* (adapted from Cox *et al.*, 2011). *Availability* was defined as a function of distance from the penguin nesting site (i.e. Humble Island), and depth, height, length, and distance to nearest neighbor. Adélie penguins concentrate their hunting dives within the top 30–40 m of the water column (Chappell *et al.*, 1993; Wienecke *et al.*, 2000). Shallower aggregations allow for a more rapid surface recovery time in diving penguins, thereby maximizing the proportion of total foraging time spent submerged (Kooyman, 1989; Chappell *et al.*, 1993). Larger aggregations are more easily seen by foraging predators and the chance of encountering larger aggregations is higher (Grünbaum and Veit, 2003). Shorter distances between

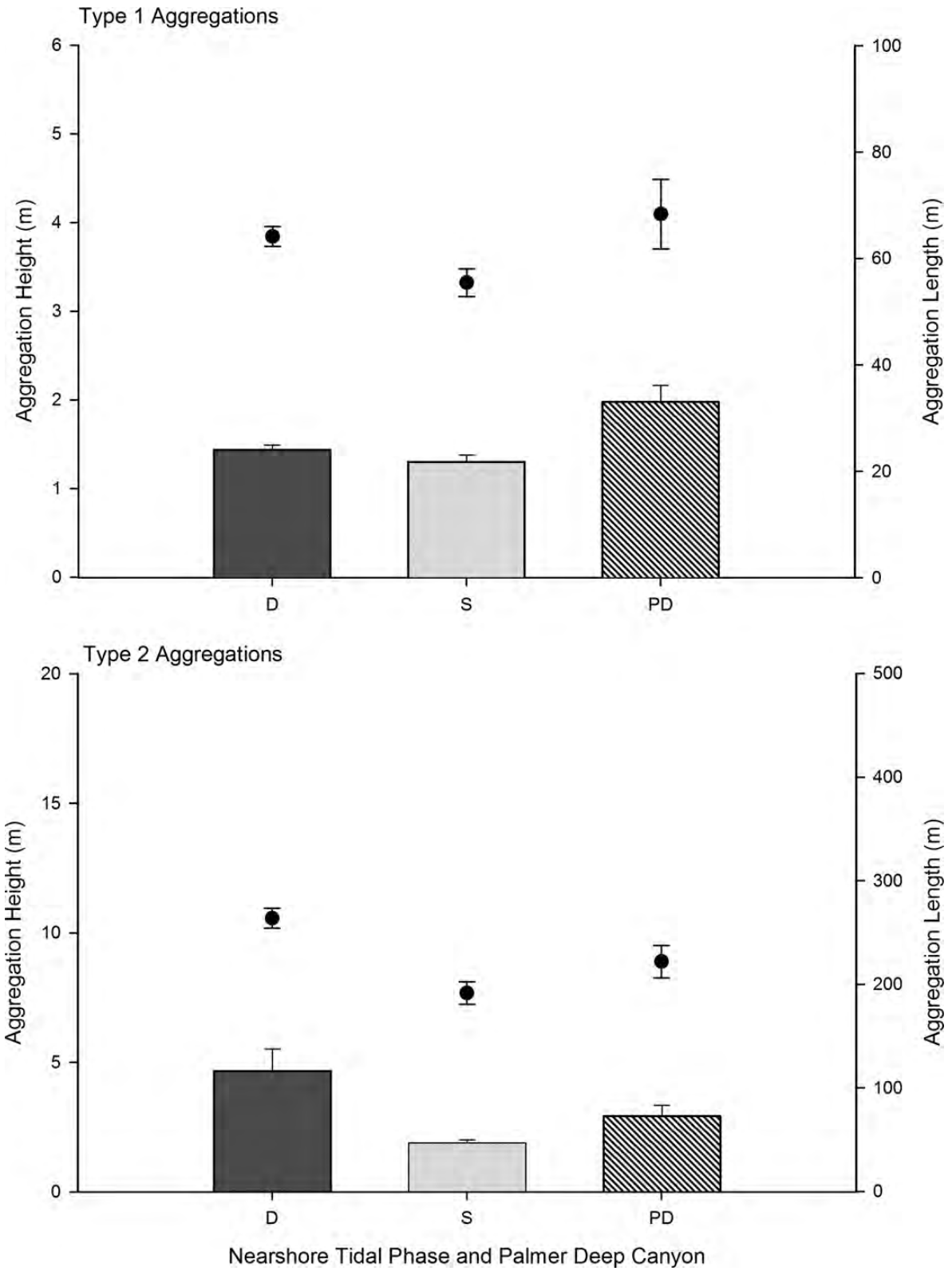

Figure 7. Mean aggregation heights (m, represented by black circles) for nearshore diurnal (D) and semi-diurnal (S) tides and for the head of the Palmer Deep canyon (PD) for Type 1 (top panel) and Type 2 (bottom panel) aggregations. Mean aggregation lengths (m, represented by bars) for nearshore diurnal (dark grey) and semi-diurnal (pale grey) tides and for the head of the Palmer Deep canyon (diagonal hatch). Error bars indicate standard errors.

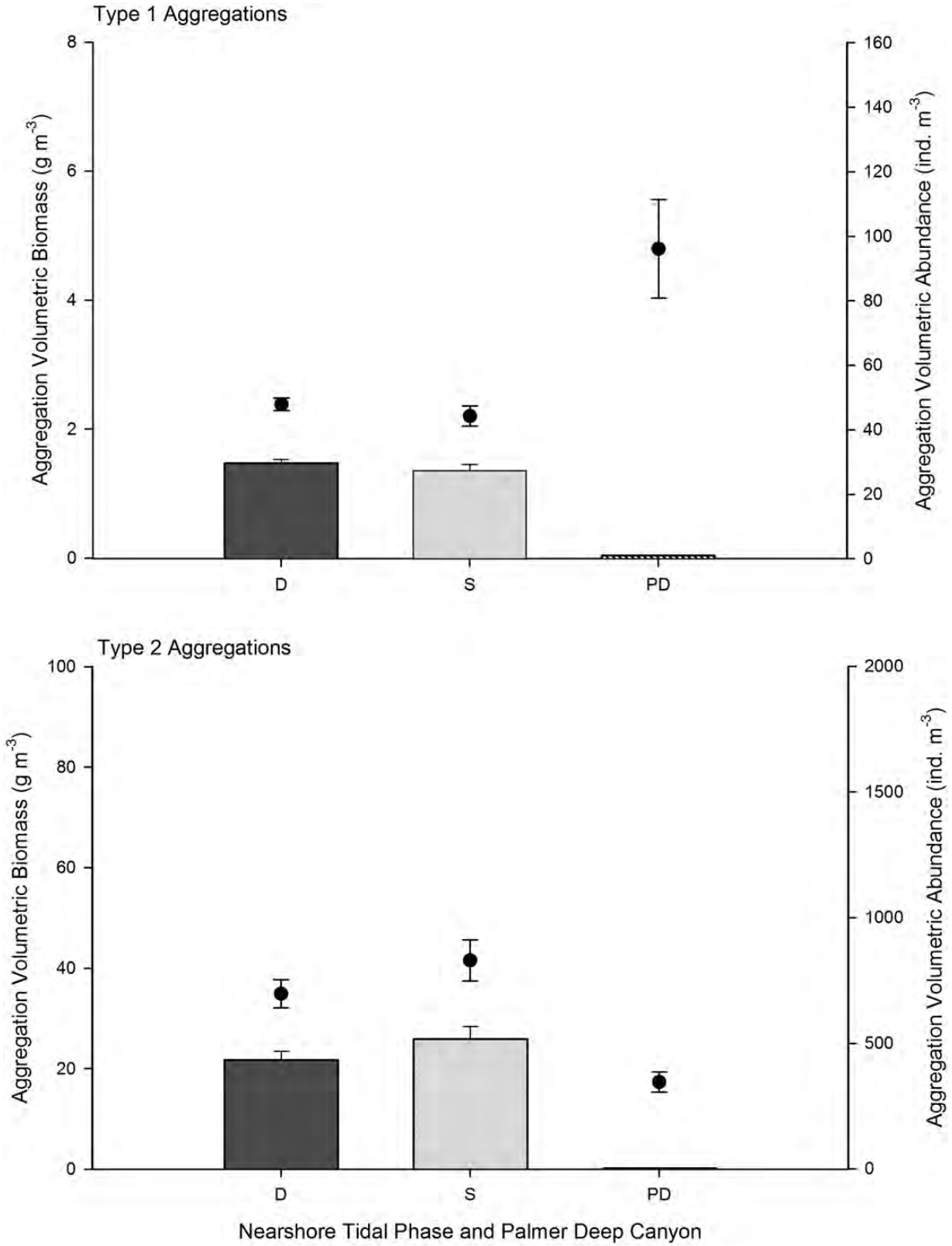

Figure 8. Mean aggregation volumetric biomass (g m^{-3}, represented by black dots) for nearshore diurnal (D) and semi-diurnal (S) tides and for the head of the Palmer Deep canyon (PD) for Type 1 (top panel) and Type 2 (bottom panel) aggregations. Mean aggregation volumetric abundance (ind. m^{-3}, represented by bars) for nearshore diurnal (dark grey) and semi-diurnal (pale grey) tides and for the head of the Palmer Deep canyon (diagonal hatch). Error bars indicate standard errors.

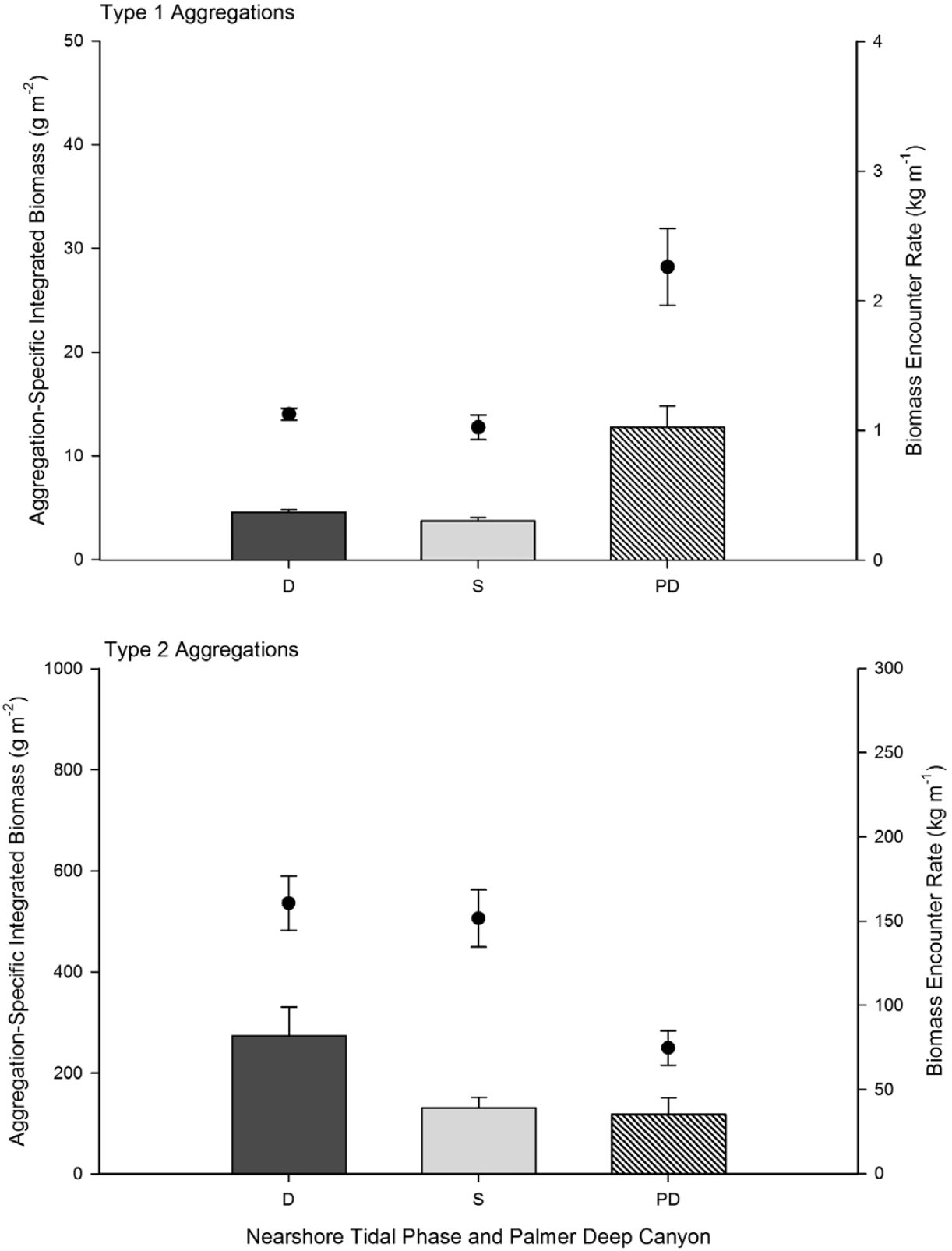

Figure 9. Mean aggregation-specific integrated biomass (g m^{-2}, represented by black dots) for nearshore diurnal (D) and semi-diurnal (S) tides and for the head of the Palmer Deep canyon (PD) for Type 1 (top panel) and Type 2 (bottom panel) aggregations. Mean biomass encounter rate (kg m^{-1}, represented by bars) for nearshore diurnal (dark grey) and semi-diurnal (pale grey) tides and for the head of the Palmer Deep canyon (diagonal hatch). Error bars indicate standard errors.

aggregations minimize searching times between hunting dives, reducing the overall time spent away from the nest or chicks. We defined *energy value* by volumetric density (both biomass and abundance), biomass encounter rate, and aggregation composition. Aggregations with greater volumetric density and biomass encounter rates will provide more nutritional value to foraging penguins. Aggregation composition refers to the age-class structure of the krill, the proportion of juveniles to mature adults, particularly gravid females; mature gravid females have the greatest energy density, represented by lipid content (Pond *et al.*, 1995).

Quality of Type 1 and Type 2 aggregations

Our Type 1 and Type 2 aggregations were distinctly different from each other; Type 2 aggregations were larger and had greater densities of krill, with higher biomass encounter rates than Type 1 aggregations. Type 2 aggregations were also shallower than Type 1 aggregations, but were further apart. If we weight the prey quality parameters for availability (size, depth, NND) and energy value (volumetric density and biomass encounter rate, but not aggregation composition since we do not have these data) equally, Type 2 aggregations can be considered as being higher quality prey than Type 1 aggregations due both to their increased availability to foraging penguins and to their higher energy value. It is more likely, however, that these parameters are not weighted equally and further research into the importance of each is required to further understand the interactions between predator and prey.

Quality of the krill prey field as related to tidal phase

Though we found a clear difference in the prey quality of Types 1 and 2 aggregations in our study, aggregation types occurred at similar frequencies irrespective of tidal phase. However, regardless of type, aggregations encountered in the nearshore during diurnal tides were shallower than they were during semi-diurnal tides. Type 1 aggregations were closer together during diurnal tides, while Type 2 aggregations had larger dimensions during diurnal tides than during semi-diurnal tides. Aggregations encountered during the diurnal tides were therefore typically more easily accessible to foraging Adélie penguins than those encountered during semi-diurnal tides, and diurnal tide aggregations can be considered as having a higher prey quality than semi-diurnal tide aggregations due to their enhanced availability to feeding penguins. Furthermore, biomass encounter rate was elevated for Type 2 aggregations during diurnal tides as opposed to semi-diurnal tides.

Quality of the krill prey field: nearshore versus Palmer Deep canyon

Aggregations encountered over the head of the Palmer Deep canyon, where Adélie penguins typically prefer to forage during semi-diurnal tides, were similar to those observed nearshore during diurnal tides in that they were more readily available to foraging Adélie penguins, despite the fact that they were further away from the nesting site on Humble Island. Palmer Deep aggregations were consistently shallower, larger, and closer together than those encountered nearshore during semi-diurnal tides. Volumetric abundances of krill in aggregations at the head of the Palmer Deep canyon were, however, orders of magnitude lower than those observed nearshore during either tidal phase. Interestingly, volumetric biomass, aggregation-specific integrated biomass, and biomass encounter rate of Type 1 aggregations were notably higher at the head of the Palmer Deep than nearshore. Aggregations at the head of the Palmer Deep canyon were thus of a higher prey quality, both in terms of availability and energy value, than those encountered in the nearshore during semi-diurnal tides.

Implications for penguin foraging

Adélie penguins are central place foragers (Orians and Pearson, 1979) and have to balance foraging time with food intake in order to ensure that their chicks are well fed and that their own metabolic requirements are met (Ydenberg *et al.*, 1994). A number of studies suggest that variability in foraging distance during the breeding season is, in part, a result of depleting krill resources nearshore (Alonzo *et al.*, 2003; Clarke *et al.*, 2006). We found that in the nearshore waters off Palmer Station, krill resources were depleted during semi-diurnal tides but then renewed again during subsequent diurnal tides. Not only did the overall densities of krill change with tidal phase, but the structure of their aggregations changed too. Aggregations encountered during diurnal tides were more readily accessible to foraging Adélie penguins than those observed during semi-diurnal tides. Apart from the extra distance required to reach the feeding grounds, krill aggregations at the head of the Palmer Deep canyon were equally accessible to diving Adélie penguins as those found in the nearshore during diurnal tides and had a higher prey quality than those aggregations encountered in the nearshore during semi-diurnal tides.

The dynamic predator–prey modelling study of Alonzo *et al.* (2003) found that penguins selecting to minimize foraging time always foraged nearshore unless krill biomass was low, in which case penguins would move further offshore. We believe that Adélie penguins nesting on Humble Island were targeting aggregations with high availability over those with high-energy value and therefore selecting to minimize foraging time over maximizing energy intake. We suggest that the alternating nearshore and offshore foraging behavior of the Adélie penguins in the waters off Palmer Station, as reported by Oliver *et al.* (2013), is in direct response to fluctuations in nearshore krill densities as well as key shifts in their aggregation structure, both of which are strongly associated with tidal phase. While Antarctic krill are well known to exhibit spatially heterogeneous distributions, our study is one of only a few (see for example Warren *et al.*, 2009) that indicate an equally high degree of temporal variability on scales from days to weeks. Not only does the overall abundance and biomass of krill vary over short time periods, but the structure of the aggregations they form vary too, with important implications for top predators.

Supplementary data

Supplementary data are available at *ICES Journal of Marine Science* online.

Acknowledgements

Our sincere thanks go to Matthew Oliver and William Fraser for sharing their early results on tidal cycle effects on Adélie penguin foraging behavior, which prompted our study. William Fraser generously provided penguin diet sample data. We thank the two anonymous reviewers for their valuable comments and suggestions for the manuscript. We are grateful to Raytheon Polar Services Company and the United States Antarctic Program for outstanding logistics, field and facilities support at Palmer Station. Special thanks go to Dominique Paxton, who assisted our research under the National Science Foundation (NSF) Research Experience for Undergraduates program. We also thank everyone else who assisted

us in the field. This is contribution number 3281 from the Virginia Institute of Marine Science, The College of William and Mary.

Funding

This study was funded by the NSF Office of Polar Programs (OPP-0823101).

References

Allen, S. E., Vindeirinho, C., Thomson, R. E., Foreman, M. G., and Mackas, D. L. 2001. Physical and biological processes over a submarine canyon during an upwelling event. Canadian Journal of Fisheries and Aquatic Sciences, 58: 671–684.

Alonzo, S. H., Switzer, P. V., and Mangel, M. 2003. Ecological games in space and time: the distribution and abundance of Antarctic krill and penguins. Ecology, 84: 1598–1607.

Atkinson, A., and Snÿder, R. 1997. Krill–copepod interactions at South Georgia, Antarctica, I. Omnivory by *Euphausia superba*. Marine Ecology Progress Series, 160: 63–76.

Bernard, K. S., Steinberg, D. K., and Schofield, O. M. E. 2012. Summertime grazing impact of the dominant macrozooplankton off the Western Antarctic Peninsula. Deep-Sea Research I, 62: 111–122.

Brierley, A. S., Demer, D. A., Watkins, J. L., and Hewitt, R. P. 1999. Concordance of interannual fluctuations in acoustically estimated densities of Antarctic krill around South Georgia and Elephant Island: biological evidence of same-year teleconnections across the Scotia Sea. Marine Biology, 134: 675–681.

Brierley, A. S., Watkins, J. L., and Murray, A. W. A. 1997. Interannual variability in krill abundance at South Georgia. Marine Ecology Progress Series, 150: 87–98.

Chapman, E. W., Hofmann, E. E., Patterson, D. L., and Fraser, W. R. 2010. The effects of variability in Antarctic krill (*Euphausia superba*) spawning behavior and sex/maturity stage distribution on Adélie penguin (*Pygoscelis adeliae*) chick growth: a modeling study. Deep-Sea Research II, 57: 543–558.

Chappell, M. A., Shoemaker, V. H., Janes, D. N., Bucher, T. L., and Maloney, S. K. 1993. Diving behavior during foraging in breeding Adélie penguins. Ecology, 74: 1204–1215.

Chu, D., Foote, K. G., and Stanton, T. K. 1993. Further analysis of target strength measurements of Antarctic krill at 38 and 120 kHz: comparison with deformed cylinder model and inference of orientation distribution. Journal of the Acoustical Society of America, 93: 2985–2988.

Chu, D., and Wiebe, P. H. 2005. Measurements of sound-speed and density contrasts of zooplankton in Antarctic waters. ICES Journal of Marine Science, 62: 818–831.

Clarke, J., Emmerson, L. M., and Otahal, P. 2006. Environmental conditions and life history constraints determine foraging range in breeding Adélie penguins. Marine Ecology Progress Series, 310: 247–261.

Cotté, C., and Simard, Y. 2005. Formation of dense krill patches under tidal forcing at whale feeding hot spots in the St. Lawrence Estuary. Marine Ecology Progress Series, 288: 199–210.

Cox, M. J., Watkins, J. L., Reid, K., and Brierley, A. S. 2011. Spatial and temporal variability in the structure of aggregations of Antarctic krill (*Euphausia superba*) around South Georgia, 1997–1999. ICES Journal of Marine Science, 68: 489–498.

Fraser, W. R., and Hofmann, E. E. 2003. A predator's perspective on causal links between climate change, physical forcing and ecosystem response. Marine Ecology Progress Series, 265: 1–15.

Genin, A. 2004. Bio-physical coupling in the formation of zooplankton and fish aggregations over abrupt topographies. Journal of Marine Systems, 50: 3–20.

Grünbaum, D., and Veit, R. R. 2003. Black-browed albatross foraging on Antarctic krill: density-dependence through local enhancement? Ecology, 84: 3265–3275.

Hunt, G. L. J., Heinemann, D., and Everson, I. 1992. Distributions and predator–prey interactions of macaroni penguins, Antarctic fur seals, and Antarctic krill near Bird Island, South Georgia. Marine Ecology Progress Series, 86: 15–30.

Kaufman, L., and Rousseeuw, P. J. 1990. Finding Groups in Data: An Introduction to Cluster Analysis. Wiley, New York.

Klinck, J. M. 1996. Circulation near submarine canyons: a modeling study. Journal of Geophysical Research, 101: 1211–1223.

Kooyman, G. L. 1989. Diverse Divers. Springer-Verlag, Berlin, Germany.

Lascara, C. M., Hofmann, E. E., Ross, R. M., and Quetin, L. B. 1999. Seasonal variability in the distribution of Antarctic krill, *Euphausia superba*, west of the Antarctic Peninsula. Deep-Sea Research I, 46: 951–984.

Lavoie, D., Simard, Y., and Saucier, F. J. 2000. Aggregation and dispersion of krill at channel heads and shelf edges: the dynamics in the Saguenay–St. Lawrence Marine Park. Canadian Journal of Fisheries and Aquaculture Sciences, 57: 1853–1869.

Laws, R. M. 1977. Seals and whales of the Southern Ocean. Philosophical Transactions of the Royal Society of London. Series B, Biological Sciences, 279: 81–96.

Lawson, G. L., Wiebe, P. H., Ashjian, C. J., Chu, D., and Stanton, T. K. 2006. Improved parameterization of Antarctic krill target strength models. Journal of the Acoustical Society of America, 119: 232–242.

Lawson, G. L., Wiebe, P. H., Ashjian, C. J., Gallager, S. M., Davis, C. S., and Warren, J. D. 2004. Acoustically-inferred zooplankton distribution in relation to hydrography west of the Antarctic Peninsula. Deep-Sea Research II, 51: 2041–2072.

Lawson, G. L., Wiebe, P. H., Ashjian, C. J., and Stanton, T. K. 2008a. Euphausiid distribution along the Western Antarcic Peninsula – Part B: Distribution of euphausiid aggregations and biomass, and associations with environmental features. Deep-Sea Research II, 55: 432–454.

Lawson, G. L., Wiebe, P. H., Stanton, T. K., and Ashjian, C. J. 2008b. Euphausiid distribution along the Western Antarctic Peninsula – Part A: Development of robust multi-frequency acoustic techniques to identify euphausiid aggregations and quantify euphausiid size, abundance, and biomass. Deep-Sea Research II, 55: 412–431.

Loeb, V. J., Hofmann, E. E., Klinck, J. M., Holm-Hansen, O., and White, W. B. 2009. ENSO and variability of the Antarctic Peninsula pelagic marine ecosystem. Antarctic Science, 21: 135–148.

Mackas, D. L., Kieser, R., Saunders, M., Yelland, D. R., Brown, R. M., and Moore, D. F. 1997. Aggregation of euphausiids and Pacific hake (*Merluccius productus*) along the outer continental shelf off Vancouver Island. Canadian Journal of Fisheries and Aquaculture Sciences, 54: 2080–2096.

Martinson, D. G., and McKee, D. C. 2012. Transport of warm Upper Circumpolar Deep Water onto the western Antarctic Peninsula continental shelf. Ocean Science, 8: 433–442.

Martinson, D. G., Stammerjohn, S. E., Iannuzzi, R. A., Smith, R. C., and Vernet, M. 2008. Western Antarctic Peninsula physical oceanography and spatio-temporal variability. Deep-Sea Research II, 55: 1964–1987.

Mauchline, J. 1980. Measurement of Body Length of *Euphausia superba* Dana. BIOMASS Handbook, No. 4. Scientific Committee Antarctic Research, Cambridge, UK. pp. 1–9.

Mori, Y., and Boyd, I. L. 2004. The behavioral basis for nonlinear functional responses and optimal foraging in Antarctic fur seals. Ecology, 85: 398–410.

Nicol, S., Clarke, J., Romaine, S. J., Kawaguchi, S., Williams, G., and Hosie, G. W. 2008. Krill (*Euphausia superba*) abundance and Adélie penguin (*Pygoscelis adeliae*) breeding performance in the waters off the Béchervaise Island colony, East Antarctica in 2 years with contrasting ecological conditions. Deep-Sea Research II, 55: 540–557.

Oliver, M. J., Irwin, A., Moline, M. A., Fraser, W., Patterson, D., Schofield, O., and Kohut, J. 2013. Adélie penguin foraging location

predicted by tidal regime switching. PLoS ONE, 8:e55163. doi:10.1371/journal.pone.0055163.

Orians, G. H., and Pearson, N. E. 1979. On the theory of central place foraging. *In* Analyses of Ecological Systems, pp. 155–177. Ed. by D. H. Horn, R. D. Mitchell, and G. R. Stairs. Ohio State University Press, Columbus, OH.

Perissinotto, R., Pakhomov, E. A., McQuaid, C. D., and Froneman, P. W. 1997. *In situ* grazing rates and daily ration of Antarctic krill *Euphausia superba* feeding on phytoplankton at the Antarctic Polar Front and the Marginal Ice Zone. Marine Ecology Progress Series, 160: 77–91.

Pond, D., Watkins, J., Priddle, J., and Sargent, J. 1995. Variation in the lipid content and composition of Antarctic krill *Euphausia superba* at South Georgia. Marine Ecology Progress Series, 117: 49–57.

Price, H. J., Boyd, K. R., and Boyd, C. M. 1988. Omnivorous feeding behavior of the Antarctic krill *Euphausia superba*. Marine Biology, 97: 67–77.

Ross, R. M., Quetin, L. B., and Haberman, K. L. 1998. Interannual and seasonal variability in short-term grazing impact of *Euphausia superba* in nearshore and offshore waters west of the Antarctic Peninsula. Journal of Marine Systems, 17: 261–273.

Sameoto, D., Wiebe, P., Runge, J., Postel, L., Dunn, J., Miller, C., and Coombs, S. 2000. Collecting zooplankton. *In* Zooplankton Methodology Manual, pp. 55–81. Ed. by R. Harris, P. Wiebe, J. Lenz, and H. R. Skjodal. Academic Press, London.

Santora, J. A., and Reiss, C. S. 2011. Geospatial variability of krill and top predators within an Antarctic submarine canyon system. Marine Biology, 158: 2527–2540.

Santora, J. A., Reiss, C. S., Cossio, A. M., and Veit, R. R. 2009. Interannual spatial variability of krill (*Euphausia superba*) influences seabird foraging behavior near Elephant Island, Antarctica. Fisheries Oceanography, 18: 20–35.

Santora, J. A., Reiss, C. S., Loeb, V. J., and Veit, R. R. 2010. Spatial association between hotspots of baleen whales and demographic patterns of Antarctic krill *Euphausia superba* suggests size-dependent predation. Marine Ecology Progress Series, 405: 255–269.

Schmidt, K., Atkinson, A., Petzke, K-J., Voss, M., and Pond, D. W. 2006. Protozoans as a food source for Antarctic krill, *Euphausia superba*: complementary insights from stomach content, fatty acids, and stable isotopes. Limnology and Oceanography, 51: 2409–2427.

Siegel, V. 2005. Distribution and population dynamics of *Euphausia superba*: summary of recent findings. Polar Biology, 29: 1–22.

Tarling, G. A., Klevjer, T., Fielding, S., Watkins, J., Atkinson, A., Murphy, E., Korb, R., *et al.* 2009. Variability and predictability of Antarctic krill swarm structure. Deep-Sea Research I, 56: 1994–2012.

Trathan, P. N., Brierley, A. S., Brandon, M. A., Bone, D. G., Goss, C., Grant, S. A., Murphy, E. J., *et al.* 2003. Oceanographic variability and changes in Antarctic krill (*Euphausia superba*) abundance at South Georgia. Fisheries Oceanography, 12: 569–583.

Warren, J. D., and Demer, D. A. 2010. Abundance and distribution of Antarctic krill (*Euphausia superba*) nearshore of Cape Shirreff, Livingston Island, Antarctica, during six austral summers between 2000 and 2007. Canadian Journal of Fisheries and Aquaculture Sciences, 67: 1159–1170.

Warren, J. D., Santora, J. A., and Demer, D. A. 2009. Submesoscale distribution of Antarctic krill and its avian and pinniped predators before and after a near gale. Marine Biology, 156: 479–491.

Wiebe, P. H., Ashjian, C. J., Lawson, G. L., Piñones, A., and Copley, N. J. 2011. Horizontal and vertical distribution of euphausiid species on the Western Antarctic Peninsula U.S. GLOBEC Southern Ocean study site. Deep-Sea Research II, 58: 1630–1651.

Wiebe, P. H., Boyd, S. H., and Cox, J. L. 1982. Avoidance of towed nets by the euphausiid *Nematoscelis megalops*. Fishery Bulletin, 80: 75–91.

Wienecke, B. C., Lawless, R., Rodary, D., Bost, C-A., Thomson, R., Pauly, T., Robertson, G., *et al.* 2000. Adélie penguin foraging behaviour and krill abundance along the Wilkes and Adélie land coasts, Antarctica. Deep-Sea Research II, 47: 2573–2587.

Ydenberg, R. G., Welham, C. V. J., Schmid-Hempel, R., Schmid-Hempel, P., and Beauchamp, G. 1994. Time and energy constraints and the relationships between currencies in foraging theory. Behavioral Ecology, 5: 28–34.

Handling editor: Stéphane Plourde